

Oxygen-sublattice ordering and intercalation mechanism of chlorine in $\text{YBa}_2\text{Cu}_3\text{O}_{6+\delta}$

E. Faulques, P. Mahot, M. Spiesser, and T. P. Nguyen

*Laboratoire de Physique Cristalline, Institut des Matériaux de Nantes, Université de Nantes,
2 rue de la Houssinière, F-44072 Nantes Cedex 03, France*

G. Garz and C. Gonzalez

*Centre National d'Etudes des Télécommunications, Laboratoire de Bagneux, 196 Avenue Henri Ravera,
Boîte Postale 107, 92225 Bagneux Cedex, France*

P. Molinié

*Laboratoire de Chimie des Solides, Institut des Matériaux de Nantes, Université de Nantes,
2 rue de la Houssinière, F-44072 Nantes Cedex 03, France*

(Received 2 February 1994)

We have investigated the modifications occurring in the oxygen sublattice and in the phonon spectra of chlorinated $\text{YBa}_2\text{Cu}_3\text{O}_{6+\delta}$ (YBCO) compounds. Susceptibility measurements suggest that the diffusion of chlorine is different in oxygen-deficient and in oxygen-rich materials. We find occurrence of superconductivity after chlorine treatment at 200 °C in an initially nonsuperconducting reduced sample. X-ray photoelectron spectra and x-ray-diffraction patterns of this sample show that the oxidation number of chlorine is between -1 and 0 in the lattice. To explain this result we assume that when an oxygen-deficient sample of approximate composition $\text{YBa}_2\text{Cu}_3\text{O}_{6.20}$ is substantially chlorinated, the chlorine enters the structure at vacancies of BaO planes and promotes the diffusion of oxygen towards empty O(1) sites of copper planes. This conclusion is supported by a comparison of vibrational results from chlorinated YBCO with those recently obtained on YBCO pristine thin films presenting oxygen-sublattice disorder and by the different magnetic behavior of chlorinated reduced and oxidized samples. A Raman resonant feature is found at 72 meV (580 cm^{-1}) and is ascribed to defect-induced modes of the oxygen sublattice rather than to electronic excitations. Indeed at 10 K, the line shapes of this band are clearly asymmetric and can be fitted using different Fano functions indicating phononic interaction with an electronic spectrum. The unusual broadening of this line on going from normal to superconducting state suggests the presence of charge-transfer excitons traveling from CuO_2 planes to CuO chains.

I. INTRODUCTION

The crucial role of oxygen stoichiometry in cuprates superconductors has created a considerable amount of work in order to understand which crystallographic sites of the oxygen sublattice are concerned with superconductivity. One way of exploring the problem is to substitute or intercalate atoms with similar chemical properties at oxygen sites. Chlorine is a good candidate for intercalation in the $\text{YBa}_2\text{Cu}_3\text{O}_{6+\delta}$ system (YBCO or 1:2:3) since its electronegativity is 3 (eV)^{1/2} on the Pauling scale and its covalent and ionic radii are 0.99 and 1.8 Å [respectively, 3.5 (eV)^{1/2}, 0.73 and 1.4 Å for oxygen]. One may argue that sulfur could be a better candidate for improving the superconducting properties since it possesses the same valence as oxygen but it appears the intercalation and treatment of YBCO with chlorine atoms is much easier and convenient because it needs fewer manipulations. Chlorination of the YBCO system was presented before in some papers. Osipyan *et al.*,¹ Pavlyukhin *et al.*,² and Radousky *et al.*³ operated with gaseous chlorine, whereas Stewart *et al.*⁴ and Myrha *et al.*⁵ used also a different route with a mixture of CuO and CuCl as starting constituents in order to achieve a better doping. In this study we have carried out systematic magnetiza-

tion and x-ray-diffraction measurements, Raman spectroscopy, and elemental analyses on two chlorinated YBCO series. In one of the series we used reduced (or deoxygenated) semiconducting samples as starting materials which then were assumed to have an oxygen sublattice restricted to the BaO and CuO_2 planes and copper layers nearly free of oxygen. In the other series we used fully oxidized (or oxygenated) superconducting starting materials thus presenting a more ordered oxygen sublattice with few vacancies in the CuO chains. The different behavior with chlorine treatment between the two series will give interesting information about the possible modifications occurring in the oxygen sublattice and resulting from chlorine insertion in the lattice. These systematic experiments include original magnetization and Raman data which were not presented before. Raman technique is particularly interesting since it deals mainly with vibrations of oxygen, an element which is difficult to trace with x-ray diffraction. We have directly probed each oxygen species to detect changes induced by chlorine insertion. In this paper we use the notation of several Raman specialists: O(1) and Cu(1) for positions of chain atoms along the *b* axis, O(4) for the apex oxygen of the BaO plane, Cu(2), O(2), and O(3) being the positions of the atoms of the superconducting CuO_2 layers. The

apex oxygen atom is often referred as the "bridge" atom between CuO chains and CuO₂ layers. Other authors note O_z and O_c the positions of the apex and chain oxygen atoms.

II. EXPERIMENT

The fully oxidized YBCO phase is prepared by solid-state reaction by mixing and grinding commercial starting constituents Y₂O₃, BaCO₃, and CuO with nominal purities 99.99%, 99%, and 99%, respectively. The ground powder is pelletized and heated at 918°C in air atmosphere for 120 h. The temperature is then lowered down to 450°C during a few hours and the pellets are finally slowly cooled down to ambient temperature. This process insures that oxygen atoms could occupy O(1) positions of the CuO chains which are thermodynamically stable. The whole procedure should be repeated three or four times to obtain pellets with good T_c and superconducting volumes and to avoid secondary phase formation.

The fully reduced semiconducting phase is obtained by heating the superconducting material at 600°C in a quartz tube under dynamical pumping during about 8 h. It is important to note that the reduced material comes from the same fully oxygenated ceramic which was deoxygenated by this procedure. Since the mixing, the grinding, and the sintering conditions are the same for both deoxygenated and oxygenated materials they have the same grain sizes, the same porosity, and the same compactness and chlorination effects in both materials will be comparative.

Chlorination of these materials is achieved by placing ceramic chunks in pyrex tubes mounted on a vacuum line (10^{-3} torr) and introducing 5×10^{-4} mol of gaseous chlorine at 1 bar. The tubes were then heated at $T_a = 150, 200, 250, 300,$ and 350°C during 150 min. After these five annealings all the pieces except those treated at 150°C were powdery indicating strong reaction with chlorine. The chlorinated reduced materials were noted CR-150, . . . CR-350 the extension indicating the annealing temperature. They are referenced as the CR series in the text. Similarly, chlorinated oxidized samples were noted CO-150, . . . CO-350 and referenced as the CO series. We also called YO6 and YO7 the pristine deoxygenated (reduced) and fully oxygenated samples. Zero-field-cooled magnetization measurements were made using a commercial SQUID magnetometer operating at 50 G. X-ray diffraction of powders was made with an Inel diffractometer using Cu $K\alpha$ radiation and data were analyzed with Prolix and U-fit softwares.⁶

The Raman spectra were recorded with a Jobin-Yvon T64000 multichannel Raman spectrometer turned in a triple subtractive monochromator configuration and equipped with a liquid-nitrogen-cooled charge-coupled device detector ensuring (i) a high signal-to-noise ratio at low-excitation power, (ii) elimination of the Rayleigh contribution at low frequencies. The samples were analyzed using several laser lines: 457.92 nm (2.708 eV) and 514.53 nm (2.41 eV) with an Ar⁺ laser, 676.44 nm (1.834 eV) with a Kr⁺ laser, both at 10 and 293 K. For low-temperature measurements we used a flowing He cryostat

and macro-Raman configuration with a laser power density of about 1 MW/m². At room temperature we used a microscope with 100× objective giving a laser spot of about 4 μm and corresponding to a power density of approximately 80 MW/m². Spectra were recorded on non-degraded samples with either unpolarized or polarized light.

Elemental analyses were carried out with energy-dispersive analysis of x rays (EDX) using a Tracor detector. Additional determination of oxygen and chlorine content was made with (i) iodometry titration, (ii) Raman spectroscopy, (iii) x-ray diffraction, (iv) argentometry and weight uptake measurements.

For x-ray photoelectron spectroscopy experiments (XPS), a ESCA LEYBOLD LH 12 spectrometer (Université de Nantes-CNRS) was used with Mg $K\alpha$ radiation at 1253.6 eV. Binding energies data were referenced to Au 4f_{7/2} line (84 eV) from a gold probe fixed on the sample holder. The chlorinated YBCO powder was deposited on a double-side adhesive tape attached to the metallic holder. Spectra of untreated YBCO recorded on solid samples were also taken for comparison purpose. The data were processed by computer with satellites and background subtraction, smoothing, and decomposition for obtainment of different components.

III. RESULTS

A. Elemental analyses

1. A-EDX analysis

The results are summarized in Table I where we indicate the atomic proportion of the Y, Ba, Cu, and Cl elements for different test specimens. The Y/Cu and Ba/Cu ratios are very near from theoretical values (0.33 and 0.66) of undoped 1:2:3 samples. When the annealing temperature is raised we note that chlorine diffuses inside the material and promotes the degradation of the crystalline structure. In CR-200, the presence of copper chloride is evidenced: since the ratio Cl/Cu is about 2/3 we may have either CuCl or CuCl₂. In CO-200 and CO-250 we have BaCl₂ presence. When T_a is raised, the chlorine proportion increases: Table I shows this effect on both reduced and oxidized chlorinated test specimen.

In particular, the results show that CR-250 has the 1:2:3 stoichiometry and contains 44–53 % of Cl atoms whereas CR-200 and CR-150 have a lesser chlorine content. In the case of CR-200, two of the four measured crystallites show secondary phases, respectively, CuCl₂ and BaCl₂. In the other crystallites, we find Y, Ba, and Cu elements roughly in the 1:2:3 proportion and a strong proportion of chlorine. In the oxidized chlorinated series CO-200 is also a 1:2:3 compound with 2–11 % of chlorine and the third measurement shows explicitly a secondary phase coexisting with the superconductor, finally CO-300 and CO-350 have 1:2:3 stoichiometry and contain roughly the same amount of chlorine with an average value of 50%.

It is seen that EDX analysis is subject to some varia-

TABLE I. EDX analysis of pristine and chlorinated samples (atomic percentages). Asterisks show secondary phases.

	YO6		CR-150			CR-200				CR-250	CR-300	CR-350
Y	15	15	8	1	2	0*	11	8	0*	7	7	Important proportion of chlorine in these compounds
Ba	35	35	25	3	32	4	23	18	33	17	12	
Cu	50	51	41	57	42	57	37	33	5	23	37	
Cl	0	0	26	39	23	39	28	41	62	53	44	
	YO7	CO-150	CO-200			CO-250*	CO-300	CO-350				
Y	13	16	14	15	2.5	0	8	11	11	8		
Ba	31	32	28	34	29	32	16	14	12	14		
Cu	55	50	46	48	7	1	29	33	23	28		
Cl	0	0	11	2.1	61	65	47	41	53	48		

tions depending on the crystallites analyzed. Therefore, other estimates of chlorine contents using either mass uptakes or chemical titration are necessary.

2. Chlorine titration

We measure the mass variations of our compounds during their thermal treatment with a microbalance of 1 μg sensitivity. The pristine material is placed in a pyrex tube already weighed and its mass is determined by subtracting the full and the empty tube. After annealing, the sealed tubes are cut and carefully weighed. Another weighing is made after cleaning the tubes. The weighing differences give the masses of the annealed materials and the number of chlorine moles inside the samples. The weighing accuracy is 2 μg .

The neutral chlorine atom has seven electrons in its external shell, but its maximum stability occurs with eight electrons. This means that chlorine completes the 3*p* subshell by the capture of one electron and becomes Cl^{-1} . However, in the YBCO crystal structure chlorine may have a mixed valency. This issue can be solved by measuring out the chloride ions with silver nitrate in acid solution and by comparing the results with the total chlorine content having reacted with the pristine material.

The chlorine titration is made by dissolving about 35 mg (accuracy of 0.01 mg) of chlorinated material in 2 cm^3 of 0.5 N nitric acid diluted in 20 cm^3 water. The $\text{Ag}^+ + \text{Cl}^- \rightarrow \text{AgCl}$ reaction is measured by pouring a volume V of $M/100 \text{ Ag}^+ \text{NO}_3^-$ in the solution with a mi-

croburet (accuracy 0.05 ml). A silver combined electrode XM950, and a reference electrode Hg_2SO_4 (0.642V) are used for the potentiometry. We measure the evolution of the potential $E_{\text{Ag}^+/\text{Ag}}$ of the silver electrode in the solution versus the volume of silver nitrate. The slope change of the $E_{\text{Ag}^+/\text{Ag}} = f(V)$ curve gives the equivalence when AgCl precipitates. Then, measurement of the corresponding silver nitrate volume gives the number of Cl^{-1} moles. The error in chloride titration is less than 2% with this procedure. We have summarized the results in Table II. Our results indicate that in the annealed materials approximately 10% of chlorine is ionic (-1 valency).

3. Iodometry

The iodometric titration was used to determine the oxygen stoichiometry of the pristine reduced $\text{YBa}_2\text{Cu}_3\text{O}_{6+\delta}$ and oxidized $\text{YBa}_2\text{Cu}_3\text{O}_{7-\delta}$ materials. The method has been described elsewhere⁷ and we found that our starting materials have the average composition $\text{YBa}_2\text{Cu}_3\text{O}_{6.29}$ (YO6) and $\text{YBa}_2\text{Cu}_3\text{O}_{6.83}$ (YO7) with a δ accuracy $\Delta\delta = 0.05$.

B. Magnetization curves

Magnetization results are summarized in Table III which gives the critical temperature, the superconducting transition width and the susceptibility at 0 K. Figure 1 presents the magnetization curves of the CO series [Fig. 1(a)] and the CR series [Fig. 1(b)]. The most important

TABLE II. Determination of Cl^0 and Cl^{-1} mole numbers in chlorinated YBCO samples from weight uptake and titration.

Compounds	CR-150	CR-200	CR-250	CR-300	CR-350
Cl_2 moles	1.75×10^{-5}	1.53×10^{-4}	1.77×10^{-4}	1.42×10^{-4}	1.57×10^{-4}
Cl^- moles	Zero	1.0×10^{-5}	2.0×10^{-5}	3.5×10^{-5}	1.2×10^{-4}
Compounds	CO-150	CO-200	CO-250	CO-300	CO-350
Cl_2 moles	2.25×10^{-5}	2.02×10^{-4}	1.86×10^{-4}	1.06×10^{-4}	1.46×10^{-4}
Cl^- moles	Zero	3.5×10^{-5}	4.05×10^{-5}	7.7×10^{-6}	8.8×10^{-6}

TABLE III. Magnetization data for superconducting chlorinated YBCO samples.

Compound	T_c (K)	ΔT_c (K)	χ (0 K) (10^{-3} emu/g)	Observations
YO7	92	5.5	-10.2	The curves show a good superconducting state for $T < T_c$. Pauli paramagnetism at $T > T_c$.
CO-150	92	4.5	-9.0	
CO-200	92	4.0	-8.4	
CO-250	92	6.0	-3.8	Deterioration of superconductivity
CR-200	92	19	-1.2	Superconductivity occurs
CR-259	92	11	-0.03	Weak superconductivity. Paramagnetic substances.

result is the occurrence of superconductivity at 92 K for CR-200. Figure 1(c) shows a magnification of the magnetization curves of nonsuperconducting CR samples. In Fig. 1(d) we have plotted the superconducting fraction differences between chlorinated samples annealed at the same temperatures and the pristine oxygenated sample.

C. X-ray diffraction

The x-ray-diffraction patterns of pristine reduced and oxidized YBCO showed sharp and intense lines characteristic of good crystalline samples. No impurity phases lines and no starting constituent lines were observed.

The patterns of the chlorinated samples recorded for all samples between $2\theta=0^\circ$ and 90° are not very intense and the lines are quite large for samples treated at $T_a > 200^\circ\text{C}$. Additionally, we found that the patterns of CR-350 and CO-350 were completely modified and that some of the peaks may characterize secondary phases resulting from reactions between chlorine and YBCO elements. The indexing of most compounds was successful since the 100-intensity line was always indexed (Table IV). It was possible to index the CR-200 superconductor using both tetragonal and orthorhombic structures. This suggests that two phases coexist in this sample. Note,

TABLE IV. X-ray-diffraction pattern indexing of pristine and YBCO chlorinated samples. Note that two phases have been found in the superconducting reduced chlorinated sample CR-200. The angle 2θ is in degrees and int is the normalized intensity.

YO6			CR-150			CR-200			tetragonal			orthorhombic		
hkl	2θ	Int.	hkl	2θ	Int.	hkl	2θ	Int.	hkl	2θ	Int.	hkl	2θ	Int.
002	14.959	6	002	14.983	6	003	22.544	40	010	22.848	32			
100	23.030	13	003	22.566	6	100	23.065	28	100	23.265	8			
101	24.255	16	100	23.046	12	101	24.218	19	011	24.068	16			
102	27.565	21	102	27.587	15	103	32.459	47	013	32.459	47			
103	32.416	100	103	32.452	100	110	32.772	100	103	32.772	100			
110	32.775	65	110	32.792	65	111	33.662	6	110	32.789	36			
112	36.192	12	005	38.038	7	112	36.244	6	111	33.767	7			
005	37.997	8	104	38.332	13	005	37.977	7	112	36.244	6			
104	38.295	14	113	40.165	13	113	40.012	25	104	38.633	21			
113	40.118	14	200	47.054	32	213	58.143	33	006	46.558	13			
200	47.020	40	116	57.663	8	220	68.703	9	020	46.676	8			
116	57.586	9	213	58.312	31				021	47.350	21			
213	58.263	33	214	62.230	6				116	58.143	33			
205	61.965	9	220	68.745	8				123	58.454	18			
206	67.858	8	303	78.089	6				213	58.699	10			
218	86.598	6	310	78.274	7				108	68.703	9			
YO7			CO-150			CO-200			CO-250					
hkl	2θ	Int.	hkl	2θ	Int.	hkl	2θ	Int.	hkl	2θ	Int.	hkl	2θ	Int.
010	22.842	10	010	22.854	10	010	22.846	10	010	22.866	12			
013	32.525	49	013	32.537	46	013	32.528	39	102	27.834	16			
110	32.800	100	110	32.816	100	103	32.795	100	013	32.560	41			
014	38.500	7	113	40.356	12	113	40.331	13	110	32.821	100			
113	40.331	14	020	40.673	20	020	46.662	18	111	33.783	7			
020	46.642	17	200	47.536	11	200	47.520	6	113	40.372	19			
200	47.503	9	123	58.223	26	123	58.201	23	020	46.706	23			
123	58.179	28	213	58.766	7	220	68.790	7	200	47.527	9			
213	58.718	10	220	68.795	12				123	58.248	34			
206	68.748	14							213	58.714	7			
128	87.207	8							108	68.800	13			

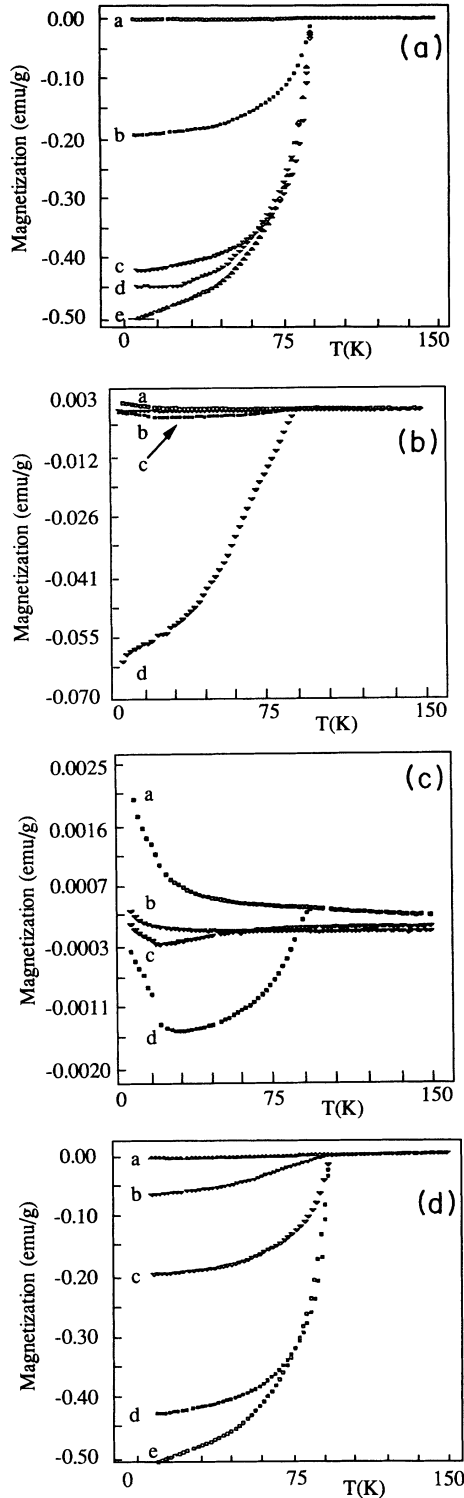


FIG. 1. Zero-field-cooled magnetization in an applied field of 50 G of (a) oxygenated $O_{6.89}$ YBCO (CO series) annealed with chlorine: (a) CO-300, (b) CO-250, (c) CO-200, (d) CO-150, (e) YO7; (b) deoxygenated $O_{6.22}$ YBCO (CR series) annealed with chlorine: (a) CR-300, (b) YO6, (c) CR-250, (d) CR-200; (c) deoxygenated YBCO (CR series) annealed with chlorine: (a) CR-300, (b) YO6, (c) CR-150, (d) CR-250; (d) YBCO (both series) annealed with chlorine at 200 and 250°C compared with pristine oxygenated material: (a) CR-250, (b) CR-200, (c) CO-250, (d) CO-200, (e) YO7.

however, that the pattern fit of CR-250 was achieved by doubling the b -cell parameter. Table V presents the a -, b -, and c -cell parameters calculated from the patterns. The c -cell parameter does not increase upon Cl doping.

D. X-ray photoelectrons results

We present in Fig. 2 the XPS results obtained on the superconducting chlorinated sample CR-200 for which superconducting occurs with chlorine treatment only. Determination of the bonding nature of ionic species in doped YBCO by this method will provide subsequent support for the discussion on the intercalation mechanism of chlorine and the resulting modifications of oxygen states.

E. Raman spectroscopy

First-order Raman scattering of the YBCO phases give phonon lines in the $0-700 \text{ cm}^{-1}$ range. In order to compare our spectra with reliable data we present the spectra obtained in the same conditions on the same machine from thin high- T_c films referenced as F 1 (H20), F 2 (Y57), and F 3 (Y42). These films were manufactured by magnetron sputtering by Garz and Gonzalez⁸ at the CNET of Bagneux and were oriented with their c axes perpendicular to the substrate. F 1 was grown on a SrTiO_3 substrate and had excellent superconducting properties: $T_{\text{onset}} = 92 \text{ K}$, $T_0 = 90.8 \text{ K}$, $\Delta T = 1.2 \text{ K}$ with a thickness of 3000 \AA . It therefore may be taken as a reference for our study. The reference spectrum of F 1 was recorded in a backscattering configuration with the incident electric field perpendicular to the c axis, i.e., lying in the a, b plane. In this particular spectrum three main bands appear at $116, 337, 498 \text{ cm}^{-1}$, with weak lines at 146 and 190 cm^{-1} , and a weak shoulder at 590 cm^{-1} . We also found other lines at $220, 410, \text{ and } 440 \text{ cm}^{-1}$ in other types of films depending on their fabrication and consequently on their oxygen sublattice ordering.⁸ The origin of these bands is given in Table VI and it should be emphasized they all stem from c -axis polarized modes, even the B_{1g} -like 337-cm^{-1} mode. We found that the spectral bands of our pristine home-handled $\text{YBa}_2\text{Cu}_3\text{O}_7$ compound (YO7) were completely coincidental with those of the F 1 reference. The 146-cm^{-1} band even ap-

TABLE V. Cell parameters of pristine and chlorinated YBCO samples.

Compound	a (Å)	b (Å)	c (Å)
YO6	3.860(3)		11.838(7)
CR-150	3.858(9)		11.824(0)
CR-200	tetragonal 3.863(0)		11.835(2)
	orthorhombic 3.822(5)	3.886(0)	11.698(8)
CR-250	3.828(8)	7.776(4)	11.711(0)
CR-300	3.822(0)	3.889(8)	11.706(6)
YO7	3.825(1)	3.890(7)	11.682(9)
CO-150	3.824(8)	3.887(5)	11.683(0)
CO-200	3.825(4)	3.888(9)	11.681(0)
CO-250	3.824(1)	3.885(9)	11.673(9)
CO-300	3.821(1)	3.887(6)	11.671(9)

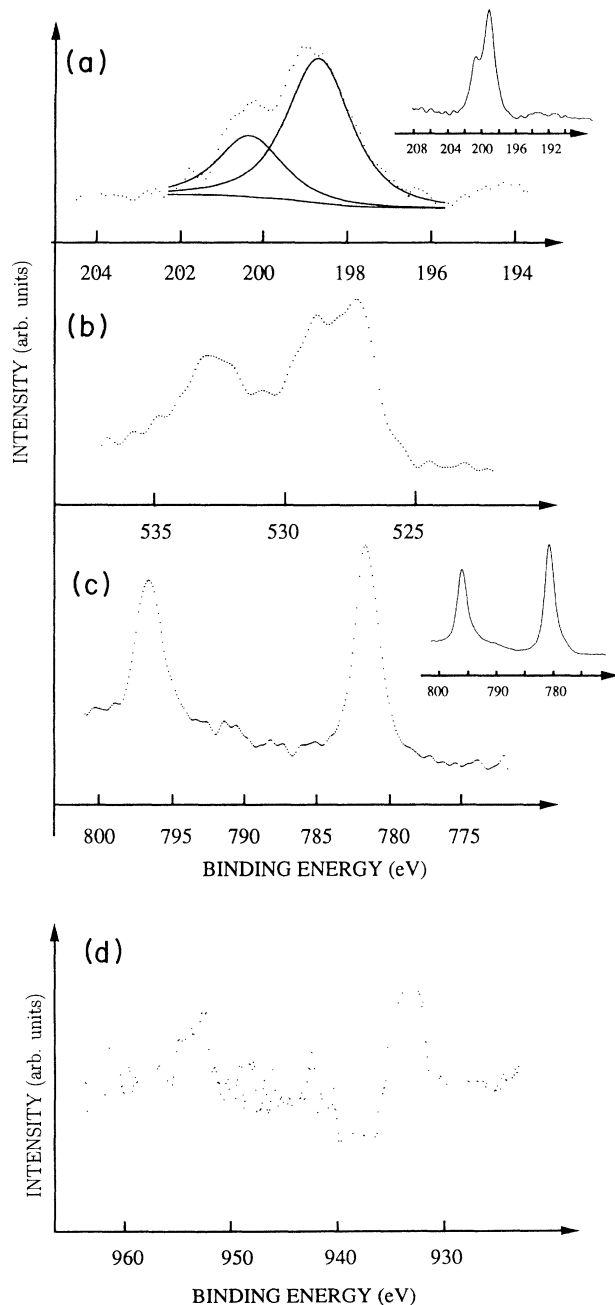


FIG. 2. XPS core-level spectra of chlorinated YBCO: (a) Cl $2p$; (b) O $1s$; (c) Ba $3d$, and (d) Cu $2p$. The insets in (a) and (c) are the corresponding spectra recorded in the BaCl_2 sample.

peared stronger whereas the intensity ratio between the 337-cm^{-1} and 500-cm^{-1} bands was almost the same. This means that our $\text{YBa}_2\text{Cu}_3\text{O}_7$ ceramic sample was of good quality as previously checked with magnetization and x-ray measurements.

Now consider the spectra obtained with the two other films F 2 and F 3 grown on MgO (001) substrates. The structural characteristics of these films may be sketched as follows. Film F 2 (Y57) was obtained at 750°C . It looked as an excellent sample with composition $\text{YBa}_{1.95}\text{Cu}_{2.95}$ and was fully oxygenated (O_7) and consequently near optimal superconducting properties were achieved with $T_{\text{onset}} = 88\text{ K}$ and $\Delta T = 3\text{ K}$. On the opposite, film F 3 (Y42) was obtained at lower temperature, 700°C , and had the cationic composition $\text{YBa}_{2.25}\text{Cu}_{3.20}$. Although its estimated oxygen content determined with Raman spectroscopy was near 6.7 it showed a broad superconductive transition with $T_{\text{onset}} = 80\text{ K}$ and $\Delta T = 22\text{ K}$. Details concerning the physical properties and the synthesis of these films have been already published in Ref. 8. The Raman spectra of F 2 and F 3 are completely different from each other [Figs. 3 and 4(e)]. Whereas the lines of F 2 are sharp and intense those of F 3 broaden with an additional feature at 580 cm^{-1} . The spectra of the chlorinated $\text{YBa}_2\text{Cu}_3\text{O}_6$ series undergo considerable changes [Figs. 4(b)–4(d)] with respect to that of the reduced pristine material [Fig. 4(a)]. The main change is the disappearance of the 337-cm^{-1} band and an intensity reduction of the 500-cm^{-1} band. The superimposition made in Fig. 4 shows that the line shape of the F 3 spectrum are close to those of chlorinated YBCO with a broadband peaked near 580 cm^{-1} . On the other hand, the spectrum of F 2 presented in this study looks like that of the reference F 1 pristine sample but a sharp mode appears at 596 cm^{-1} .

Additionally, the spectrum of the pristine $\text{YBa}_2\text{Cu}_3\text{O}_{6.2}$ reduced compound does not exactly exhibit the same features as that of the $\text{YBa}_2\text{Cu}_3\text{O}_7$ material. In our O_6 compound bands are found at $143, 220, 280, 337, 448,$ and 560 cm^{-1} [Fig. 4(a)]. Finally, the spectra of two oxidized chlorinated superconductors (CO-200 and CO-350) were recorded. They also exhibit a broad feature around $560\text{--}580\text{ cm}^{-1}$ which should be of the same nature as that observed for film F 3 and for chlorinated reduced samples. Our $\text{YBa}_2\text{Cu}_3\text{O}_{6.2}$ spectrum can be compared to that obtained by Burns *et al.*⁹ on a reduced YBCO single crystal where three lines at $125, 140,$ and 600 cm^{-1} occurred with no visible structure near 500 cm^{-1} . It is im-

TABLE VI. Raman lines (cm^{-1}) of the $\text{YBa}_2\text{Cu}_3\text{O}_7$ phase and assignment.

Frequency	Assignment
114	A_g , Ba
140	A_g , Cu of CuO_2 plane
190–220	Defective mode associated with mode at 590 cm^{-1}
337	B_{1g} -like, O(2,3) of CuO_2 plane, out-of-phase motion
430	A_g , O(2,3) of CuO_2 plane, in-phase motion
496	A_g , O(4) of BaO plane, apex oxygen, in-phase motion
$\approx 560\text{--}570$	B_{1g} O(4) or O(1) defective mode
$\approx 590\text{--}600$	A_g O(4) or O(1) defective mode

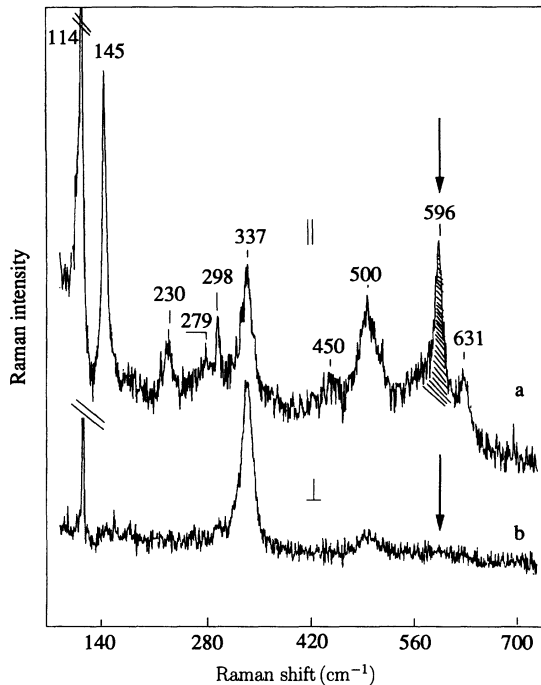


FIG. 3. Raman spectra of a YBCO thin film (F 2, Y57) fully oxygenated with weak oxygen disorder. Polarization \parallel (a) and \perp (b). The defect-induced mode is dashed.

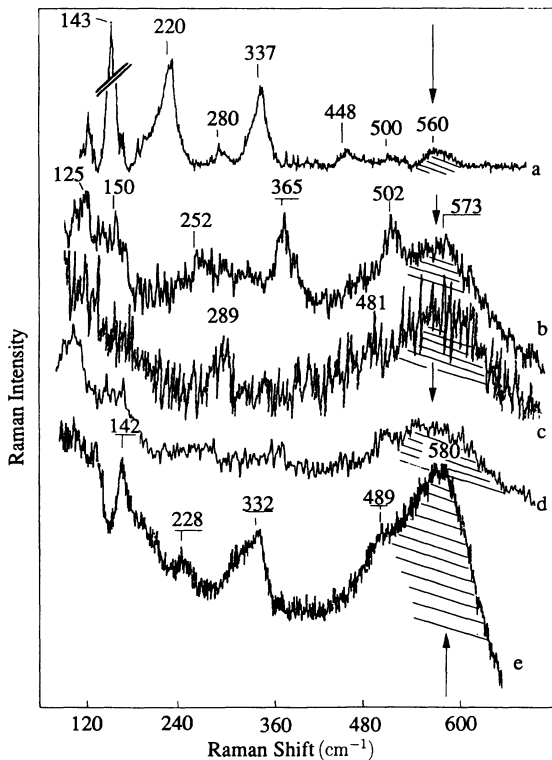


FIG. 4. Raman spectra of the pristine reduced YO6 sample (a), the same sample annealed with chlorine at 150°C (b), at 200°C (c), at 300°C (d). The spectrum of a pristine superconducting strongly disordered YBCO (film F 3, Y42) is shown by curve (e). The dashed bands are induced by defects and oxygen sublattice disorder. Unpolarized scattered light. Not smoothed.

TABLE VII. Raman lines (cm^{-1}) of BaCl_2 and CuCl_2 .

BaCl_2		CuCl_2	
32	152	66	289
50	159	110	408
59	253	216	
82	425	235	
122	533		
133		248	

portant to note that secondary phases like CuO , Y_2O_3 , Y_2BaCuO_5 , BaYO_4 , BaCuO_2 give well-known spectra with relatively intense bands compared to those of the superconductor. We have also recorded the Raman spectra of BaCl_2 and CuCl_2 which are the most probable secondary phases present in chlorinated YBCO. Their lines frequencies are listed in Table VII. The Raman signatures of all these phases cannot be found in spectra of chlorinated YBCO in contrast to what can be seen, for example, in Fig. 9(a) of Ref. 10.

IV. DISCUSSION

A. Magnetization and x-ray-diffraction data

The reaction kinetics of chlorine in YBCO sintered ceramics is rather fast since the samples have completely reacted after 150 min and reaction begins only for temperatures higher than 150°C according to Radousky *et al.*³ Magnetization data show that there is no difference between pristine samples and those annealed at 150°C but drastic evolution above this temperature for both series, reduced (or deoxygenated) and oxidized (or oxygenated) samples.

The EDX analysis shows a drastic increase of chlorine content when T_a is raised. There are several assumptions which explain this result: (i) the chlorine atoms diffuse on O(1) vacancies of the reduced $\text{YBa}_2\text{Cu}_3\text{O}_6$ structure, (ii) substitute oxygen atoms of BaO planes in $\text{YBa}_2\text{Cu}_3\text{O}_6$ and in $\text{YBa}_2\text{Cu}_3\text{O}_7$, (iii) or they can be sorbed at the grain boundaries which is consistent with the high content of chlorine in CR-150. The chemical analysis of chlorine has evidenced a proportion of Cl^{-1} not negligible (10%). This anion is too large (1.81 Å) to occupy an oxygen site (1.40 Å) in the YBCO structure. To accommodate Cl in the structure without modifying the c -cell parameter the only way is to consider that its ionic radius is reduced with a charge state between -1 and 0 . In all cases it is difficult to determine the exact stoichiometry of intercalated chlorine. Additionally, it is also difficult to consider that chlorine could substitute for oxygen atoms of the CuO chains since its oxidation number would be near -2 which seems unrealistic from the present results. A much better assumption respecting a valency of -1 for chlorine would be to consider the possible formation of ClO^- or ClO_2^- bound species.

Barium layers are expected to present vacancies since it was shown by ion channeling experiments that O(4) apical atoms may move towards other sites.¹¹ This would explain why superconductivity occurs in the oxygen-

deficient $O_{6.2}$ phase chlorinated at 200°C since electrons in excess or charge-transfer excitons resulting from $(O-O)^{2-}$ holes pairing¹² in the CuO_2 layer could easily be pumped by chlorine if it is intercalated in BaO planes. In particular, the formation of the ClO^- moiety between the barium layer and the Cu layer is highly possible via CuOCl bonding. On the other hand, the action of chlorine on fully oxygenated superconducting CO samples is easily understandable and should come from a different process: chlorine should take excess oxygen in CuO chains and then lower gradually the superconducting volume when T_a increases promoting the formation of an insulating phase with a near oxygen-deficient O_6 composition which is maximum for CO-300 and CO-350. This process should involve the total amount of oxygen present in the chains for each temperature, since there is no continuing variation of T_c with T_a , but always the same 90-K transition. The magnetic properties of the bulk material would only depend on the quantity of superconductor having not reacted with chlorine due to a diffusion kinetics of chlorine inside the material. This is easily checked by reckoning the superconducting fraction

$$f_s = \frac{\chi_{0\text{K}}(\text{doped})}{\chi_{0\text{K}}(\text{pristine } O_7)}$$

in each of the CO samples. Figure 1(a) gives immediately $f_s = 90, 84,$ and 40% of superconducting phase for CO-150, CO-200, CO-250, respectively, the other sample CO-300 is insulating as well as CO-350 which data points are superimposed with those of CR-300.

From Figs. 1(a) and 1(c) we observe that the starting material $YBa_2Cu_3O_{6.2}$ and the compounds CR-150, CR-300, CR-350, CO-300, and CO-350 are not superconducting. It can be seen that YO6 and CR-150 and CR-300 and CR-350 (not shown here) contain paramagnetic secondary phases. CO-300 and CO-350 have a zero magnetic moment per unit volume.

These results give interesting information concerning the temperatures T_a at which chlorine reacts with YBCO. For $T_a \leq 150^\circ\text{C}$ the magnetic properties do not vary, for $150 \leq T_a \leq 250^\circ\text{C}$ we obtain superconducting samples whatever the initial oxidation state of the material. For $T_a > 300^\circ\text{C}$ the superconducting (SC) state is destroyed and a disordered structure prevails. The superconducting fraction f_s is reduced for the oxidized series whereas superconductivity appears in the CR-200 sample which exhibits a smaller f_s than in oxygenated CO superconductors. However, superconductivity of the reduced CR series is destroyed above 200°C. The CR-250 sample exhibits a Curie tail [see magnification in Fig. 1(c)] which is certainly due to paramagnetic Cu^{+2} cations. In this sample a beginning of superconducting transition is clearly seen around 92 K and can be easily explained if we consider that its magnetization results from the superimposition of two signals coming from the superconducting phase and from an insulating phase. Indeed, if we look at the magnetization curves of the CR-200 and of the CR-300 samples, we can deduce the amount of superconducting phase present in the CR-250

sample. Since susceptibilities add linearly, we have $\chi_{CR-200} = (1 - f_s)\chi_{CR-300}$ where f_s is the superconducting fraction in CR-250 and $\chi_{CR-250}, \chi_{CR-200},$ and χ_{CR-300} are the susceptibilities of CR-250, CR-200, and CR-300, respectively. We find that CR-250 contains 6.2% of superconducting phase which explains the onset of superconducting behavior near 92 K.

The magnetization data of those samples which are superconducting show a constant T_c around 90 K. Suppose that chlorine occupies O(1) oxygen vacancies. We then should have a charge transfer from CuO_2 planes towards Cl at O(1) sites. However, we know that T_c depends on the concentration of peroxitons or $(O-O)^{-2}$ holes in CuO_2 planes which cause the charge transfer. Chlorine is also less electronegative than oxygen. We should then obtain different T_c values for the pristine and annealed chlorinated samples which is not the case in the present study. Then the chemical nature of the CuO chains is expected to remain unchanged in agreement with the fact that insertion of Cl^{-2} at O(1) sites is possibly not the right mechanism. It is more likely that chlorine could be inserted in the lattice as bound species like ClO^- . In the superconducting CR-200 sample we believe that chlorine promotes the migration of oxygen atoms from either BaO or CuO_2 layers towards vacancies of the oxygen-deficient Cu layer. Since the electronic affinity of chlorine is much stronger for barium than for copper, it is likely that the oxygen diffusion comes from BaO layers and that chlorine could occupy O(4) sites. Such a process would change the Ba cation's environment which will be discussed below from XPS measurements. The evolution of the superconducting fraction f_s in the CR series especially at 200°C where the material is a good superconductor can be explained by such a process explaining the observed f_s increase.

We also observe a drop of f_s in the chlorinated $YBa_2Cu_3O_7$ phases. This should be explained as a result of a diffusion of chlorine inside the material which reacts with the structural elements as seen from EDX data and therefore deteriorates the structure. For all oxidized chlorinated samples the f_s value of the fully oxidized phase cannot be reached.

Another remark concerns the superconducting transition width ΔT which can give some information on the texture of the materials. First, the Curie tail observed in CR-250 comes from a Cu^{+2} paramagnetism originating certainly from $CuCl_2$ which obeys the $1/T$ Curie law. This secondary phase does not appear for $T_a = 350^\circ\text{C}$. Second, for low temperatures the grain boundaries act as Josephson junctions.⁷ When these junctions are established, the magnetic field can enter the material up to the London penetration depth, but when the temperature is raised, the intergrain coupling decreases, the flux lines penetrate the grains and decrease both the strength of the Meissner effect and the superconducting fraction. In thin powders the intergrain junctions are weaker since the superconducting volume is related to the grain size. Therefore, the larger the transition width the weaker the intergrain coupling. When T increases the large ΔT may also come from an increase of secondary phases response to

the detriment of the superconducting phase. We observe that ΔT does not vary very much for the CO series whereas in the CR series it is larger and maximum for CR-200 where superconductivity occurs. Since the oxygenated and deoxygenated phases are assumed to have the same textural properties the different ΔT behavior in both series certainly comes from different kinetics of chlorine diffusion at the grain boundaries and inside the grains. The large ΔT in the chlorinated superconducting CO series cannot be related to the size of the grains but rather to a chlorine diffusion at the grain boundaries which breaks the intergrain links and makes the material brittle.

It is interesting to correlate magnetic data with the structure of the cationic sublattice determined from the XRD refinements. The CR series is tetragonal up to CR-200 where superconductivity appears and then orthorhombic for samples annealed above 200 °C. This result is in sharp contrast with that of the CO series which is orthorhombic. The calculations show higher a and c parameters in pristine reduced YBCO indicating good reduction and poorer oxygen content as expected from the synthesis. The only choice to index the chlorinated CO series is an orthorhombic unit cell, in agreement with the superconducting properties of these samples. However, the superconducting CR-200 sample can be indexed using both tetragonal and orthorhombic structures, this is an indication that at least two superconducting phases may be present in this sample.

A very important observation to be made is that there is no increase of the c parameter upon chlorination, on the contrary this parameter decreases noticeably in the case of the reduced chlorinated series from about 1.2% (up to 0.14 Å of compression). The c parameter does not change so abruptly for the chlorinated oxidized series (0.09%). Therefore, there should be no intercalation of chlorine between the different layers of YBCO contrary to the case of bismuth cuprates doped with iodine¹³ (but intercalation inside the layers is possible). More important, the ionic radius of chlorine does not apparently exceed that of an oxygen ion which confirms that its electric charge should be less than or equal to 1 as previously suggested.

The oxygen content of pristine materials can be determined with x-ray data. Pavlyukin² has shown that there is a direct correlation between the cell parameters and δ :

$$\delta = 1.5 - 65 \left[\frac{c}{3\sqrt{ab}} - 1 \right].$$

We then find the composition of our ceramics to be $\text{YBa}_2\text{Cu}_3\text{O}_{6.04}$ and $\text{YBa}_2\text{Cu}_3\text{O}_{6.88}$ with a $\Delta\delta = 0.1$ accuracy. The oxygen content for the reduced material seems to be too low since it is extremely difficult to achieve the O_6 stoichiometry.

Let us focus now on the result of the EDX analysis of the chlorinated reduced sample which shows superconductivity (CR-200). If we account for the presence of secondary phases in this sample namely BaCl_2 and CuCl_2 it is clear that they are not completely detrimental for superconductivity since this is the only superconducting

sample of the reduced series. Moreover, the presence of these phases in the two CR-200 crystallite measurements showed by the entries of Table I cannot account solely for the measured chlorine content. The first crystallite has the $\text{Y}_1\text{Ba}_{2.09}\text{Cu}_{3.33}\text{Cl}_{2.56}$ composition whereas the second one has the $\text{Y}_1\text{Ba}_{2.39}\text{Cu}_{4.46}\text{Cl}_{5.31}$ stoichiometry. Barium and copper in excess may come from secondary phases and give a chlorine molar composition of 0.84 (0.66+0.18) and 3.62 (0.8+2.92). As we can see, we then have a molar composition of $2.56 - 0.84 = 1.62$ and $5.31 - 3.62 = 1.69$ for the remaining chlorine which cannot come from BaCl_2 or CuCl_2 but is rather inserted in the YBCO lattice. We thus estimate the average stoichiometry of these chlorinated crystals to be near from $\text{YBa}_2\text{Cu}_3\text{O}_{5.4}\text{Cl}_{1.6}$ if chlorine enters at oxygen vacancies.

B. Available XPS data

Figure 2 shows the core-level spectra of different elements for the superconducting chlorinated YBCO sample. The O 1s signal presents two distinct peaks located at 531.9 and 527 eV, respectively. The latter is actually a manifold of peaks which can correspond to inequivalent oxygen lattice sites. Earlier studies on high- T_c materials¹⁴ have suggested that the peak at higher energy would be related to extrinsic or contamination oxygen. However, in a series of bismuth high- T_c materials analyzed by XPS,¹⁵ we have found that this peak is essentially intrinsic because it is always present in freshly cut samples just before analyses. The results obtained in high- T_c materials by many other workers corroborates the nature of these compounds.¹⁶ We focus our discussion on the peak found at lower binding energy and particularly on its low value (527 eV). As a matter of fact, previous XPS studies on YBCO materials have established that this peak is found in a range of 528–529 eV. Some recorded spectra revealed that a shoulder at 527 eV is formed in the O 1s spectrum.¹⁷ Using second derivatives of the spectra, Vasquez *et al.*¹⁸ have demonstrated that the actual intrinsic line is composed of two peaks located at 528 and 527.1 eV which originate from the CuO chains and CuO_2 planes. In an earlier work, Weaver *et al.*¹⁹ have suggested this possibility by deconvoluting the O 1s spectrum of several 1:2:3 compounds. It is interesting to note that in chlorinated YBCO, the enhancement of the O 1s spectrum occurred at lower binding energy part. This suggests then an increase of oxygen ordering in CuO chains. Concurrently, a higher valency of copper (> 2) would be observed. This is effectively happened in the Cu 2p spectrum where the main peak is recorded at 934.4 eV. Comparing this value to those obtained on common high- T_c materials and from the shape of the Cu 2p line, we estimate that both Cu^{II} and Cu^{III} oxidation states are present in our samples.

The presence of chlorine was detected by the Cl 2p line showing the $2p_{3/2}$ component at 198.7 eV and the $2p_{5/2}$ component at 200.3 eV. Deconvolution of the spectrum gives 2:1 doublet and makes evidence of the single saturated environment of chlorine. The oxidation state of the chlorine species is estimated to be less than unity

from the relative binding-energy value in comparison with Cl^- or C-Cl [with peak position for Cl $2p$ line at 200.3 eV (Ref. 20)]. The Ba $3d_{5/2}$ line located at 781 eV corresponds to two valent Ba as commonly observed in Ba oxide²¹ and the Y $3d_{5/2}$ line (not shown) is found at 157.5 eV which can be ascribed to unreacted Y_2O_3 .²¹ We notice that the Ba spectrum does not show peak at high binding energy as observed in contaminated YBCO,²² which is obviously consistent with a single chemical state in the analyzed samples. On the other hand, analysis of BaCl_2 standard shows that Ba $3d_{5/2}$ peak appears at 780.6 eV and Cl $2p$ peak at 198.7 eV [inset of (a) and (c)] which are in good agreement with the results reported by Vasquez.²³ The similarity of the peak position of chlorine may suggest that BaCl_2 would be formed upon doping.

C. Raman data

Raman spectroscopy is a technique sensitive to variation of electronic susceptibility in crystals since in Stokes-Raman scattering process phonons are created with small crystal momentum and modulate the scattered electric field. Interaction between phonons and collective electron excitations can be observed as changes in scattering intensity and line shapes, especially in superconductors. According to the standard Bardeen-Cooper-Schrieffer scheme boson condensation appears at $T < T_c$ and strongly correlated electronic pairs prevail over. When photons with energy greater than pairing energy interact with the material the pairs relax and contribute to an electronic scattering continuum. When pairs are relaxed to Fermi states this continuum develops as a broad peak in the Raman spectrum which can distort phonon line shapes. Therefore, it is possible to derive values of superconducting gap and electron-phonon coupling parameters from those spectra. However, the nature of correlated pairs is still not established in high- T_c materials. Phonon Raman spectra of copper-oxide superconductors are known to be very weak especially when recorded in the SC state. This weakness is due for the most part to the fact that the exciting electric field vanishes at the surface of the material owing to its metallic-like behavior.

An interesting contribution of Raman spectroscopy is the possibility to observe directly the oxygen vibrations in the structure²⁴ and to probe oxygen content of YBCO phases and oxygen local site coordination. Thus, this technique can be used for sensitive analysis of vacancies and defects in the oxygen sublattice. For instance, it has been recently evidenced that microstructural domains of orthorhombic O_I (O_7), O_{II} ($\text{O}_{6,5}$), and tetragonal T (O_6) phases coexist in poorly oxygenated YBCO single crystals.²⁵

It was shown that the frequency ω of the Raman band originating from the apex oxygen vibration is strongly dependent on the oxygen content. This variation originates from the variation of the c -cell parameter with δ : there is a contraction of the unit cell due to the reduction of the c parameter when the oxygen content increases and

therefore the c -axis polarized Raman mode of the apex oxygen may vary in frequency and is shifted upwards as a result of Cu(2)-O(4) bond hardening. Feile²⁶ has reviewed the Raman works on YBCO and was able to give an empirical relation between ω and the total oxygen content x . This relation can be expressed as

$$x = 0.037\omega(x) - 11.555 .$$

The accuracy Δx with this method is about 0.05, i.e., better than with x rays. It should be emphasized that usage of the O(4) vibration frequency for the determination of the oxygen content was obtained from earlier measurements of oxygen-deficient pristine samples. Therefore, since a chemical modification by chlorine in the present samples has strong effect on the vibrational spectrum application of this method is certainly not very well adapted if chlorine substitutes for apex or chain oxygen atoms. Indeed, there is a lack of a measurable Raman line around 500 cm^{-1} [the O(4) apex mode] in some of our chlorinated samples which did not permit the determination of x . In particular, it was almost impossible to find this apex oxygen Raman band in the CO series. This is understandable if chlorine diffuses into BaO planes to substitute for oxygen atoms and to react with barium as shown with EDX analysis. Nevertheless, we find that the starting oxygenated material has the composition $\text{YBa}_2\text{Cu}_3\text{O}_{6.89}$ since $\omega = 498 \text{ cm}^{-1}$. The lack of the O(4) band in the unpolarized spectrum of the reduced pristine material is in favor of an oxygen-deficient $\text{YBa}_2\text{Cu}_3\text{O}_6$ composition. This is in agreement with x-ray absorption and it should be noted that three methods (iodometry, x-ray, and Raman measurements) give the same x in the oxygenated sample. However, some of the spectra of the reduced chlorinated CR series exhibit undoubtedly the apex mode which has measurable frequencies. Taking into account the above restriction concerning the determination of oxygen content in these modified ceramics, we find that some of the investigated microcrystals could have an oxygen content of 7 for CR-150 ($\omega = 502 \text{ cm}^{-1}$), 6.26 ($\omega = 481 \text{ cm}^{-1}$) for CR-200, and 7 for CR-300.

The structural changes in reduced chlorinated materials which are partially observed from x-ray patterns should have an influence on the vibrational spectrum. Focus on the spectra of thin films F 2, F 3 and of chlorinated samples (Figs. 3 and 4). Depending on the synthesis conditions we have additional vibrational features appearing in the $190\text{--}220 \text{ cm}^{-1}$ and $560\text{--}600 \text{ cm}^{-1}$ spectral ranges and in the case of F 3 a complete modification of the spectrum characterizing the pristine O_6 and O_7 phases.

The nature of the 580-cm^{-1} broad line appearing in both disordered and chlorinated systems may be either (i) electronic or (ii) phononic. The first scenario may receive strong support from recent experiments and calculations of Chen *et al.*²⁷ who found broad profiles in fully oxidized YBCO crystals with widths similar to those reported in our study. They were able to fit these profiles with a theoretical Raman spectrum including a pure electronic continuum. However, (i) the line-shape maxima vary

strongly with the oxygen content, from 470 cm^{-1} for an O_7 crystal to 550 cm^{-1} for an $\text{O}_{6.97}$ crystal, (ii) the line shape is asymmetric but reversed with respect to that of our compound, namely, the lower-frequency portion of the profiles decreases steeply and the higher-frequency side has a smooth tail, (iii) their spectra have clearly B_{1g} symmetry contrary to our case where the spectrum is A_g , (iv) the peak position for the $\text{O}_{6.97}$ compound seems to be too low compared with our values even if we may suppose that this location would be upshifted to 580 cm^{-1} for an $\text{O}_{6.83}$ crystal, (v) finally the line observed by Chen only appeared at low temperature.

In the second scenario we assume that this feature is phononic and stems either from the oxygen O(1) atoms of CuO chains^{9,28–30} or from the oxygen O(4) apex as suggested from recent shell-model calculation³¹ and from polarized single-crystal experiments.^{9,32} In the first case, this vibration should be inactive in Raman since the O(1) chain atom is on an inversion center but may be allowed if the crystal centrosymmetry is lost due to crystalline changes, i.e., if the O(1) site symmetry is C_{4v} or C_{2v} . In other words it could be an infrared mode activated in Raman. This assumption is strongly supported by earlier observations made by Kuzmany *et al.*³³ and Guettler *et al.*³⁴ of a mode near 580 cm^{-1} in IR spectra of pristine YBCO and in Raman spectra of iodinated YBCO.¹³ Another evidence of the existence of a phonon in this region was given by the measurement of the generalized phonon density of states $G(\omega)$ at 6 K for both $\text{YBa}_2\text{Cu}_3\text{O}_7$ and $\text{YBa}_2\text{Cu}_3\text{O}_6$. In addition to intense features peaked at 80, 121, 180, 338, 410 cm^{-1} , a strong peak was found at 565 cm^{-1} (70 meV), its intensity being stronger for $\text{YBa}_2\text{Cu}_3\text{O}_6$.³⁵ This 580-cm^{-1} band may also arise from apex oxygen O(4) vacancies. Indeed, shell-model calculation predict a vibrational mode induced by apex vacancies-apex oxygen coupling near 590 cm^{-1} , i.e., upshifted by 90 cm^{-1} with respect to the apex oxygen mode.³¹

Raman experiments on several other thin high- T_c films with various oxygen sublattice orderings were made previously by us.⁸ In the frame of the phonon-induced picture we believe there could be several different modes in the $560\text{--}600\text{ cm}^{-1}$ range and at least two of them clearly visible for these films at 569 and 596 cm^{-1} . We may figure out that these modes could stem from defects of different nature. It is remarkable that the 596-cm^{-1} mode of the weakly disordered film F 2 appears to be very strong in parallel polarization (\parallel) whereas it is lacking in the crossed polarization (\perp) spectrum and thus may have an A_{1g} -type symmetry as for all other modes except the 337-cm^{-1} line (Fig. 3). The important point under consideration in the present work is that the Raman spectra of chlorinated samples from both CR and CO series are surprisingly similar to those recorded on thin films like F 3. From x-ray studies it is known that F 3 exhibits good cation ordering⁸ so that its perturbed Raman spectrum should arise only from oxygen disorder.

It is worth noting that the 580-cm^{-1} band may correspond to a phonon density of states (PDOS). If it is a PDOS there should be no vacancies ordering in chlorinated samples since we would instead obtain a thinner

Lorentzian band near 596 cm^{-1} as for thin film F 2. We could have direct evidence that chlorine interacts with either BaO planes or CuO chains whatever the starting material since the specific Raman response of these structural elements is strongly perturbed.

Figure 5 shows that a strong electronic Raman scattering was emitted by the superconducting chlorinated sample when recorded with $\lambda=457.92\text{ nm}$ (2.708 eV) underlying strong spectral features at 121 and 595 cm^{-1} which we believe are phononic and not electronic. The 595-cm^{-1} band does vanish in crossed polarization and then is of A_{1g} nature whereas the B_{1g} 332-cm^{-1} mode is enhanced as expected from selection rules. The presence of a weak 494-cm^{-1} A_g mode in this spectrum shows that these selection rules are not completely fulfilled which is in agreement with strong disorder in the oxygen sublattice of CR-200. It seems also that a spectral component remains at 560 cm^{-1} which would characterize another defect mode with B_{1g} symmetry.

At low temperature our measurements show an electronic continuum for all samples investigated. In the case of the oxygen-disordered film F 3 (Y42), a line-shape asymmetry of the 580-cm^{-1} phonon recorded for the $\lambda=676.4\text{ nm}$ excitation line is clearly evidenced and looks extremely strong [Fig. 6(a), spectrum a]. No satisfactory spectrum was obtained with the same excitation line for CR-200 at 10 K, but we succeeded recording a spectrum with $\lambda=514.53\text{ nm}$ [Fig. 6(b)] at 10 K which exhibits clearly an asymmetric line shape as in the case of film F 3. The observation of the 580-cm^{-1} feature for three exciting laser lines covering the entire visible spectrum from 1.834 to 2.708 eV is an indication of its resonant character.

The asymmetric shape of this feature may be calculated using the Fano interference model.³⁶ Application of

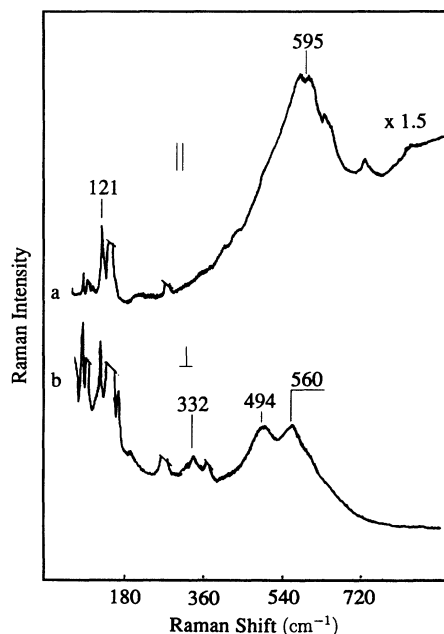


FIG. 5. Raman spectra of the reduced chlorinated superconducting sample (CR-200) recorded with the 457.9-nm laser line, polarization \parallel (a) and \perp (b) at room temperature.

this model to experimental data shows that there should be a coupling between a background continuum spectrum arising likely from electronic scattering and the phonon exhibiting an asymmetric shape. To perform the fit of this oxygen-defect-induced mode, we used a scaled Fano function $(F - s)/t$ with F defined as

$$\frac{(\omega - \omega_p + q\Gamma)^2}{(\omega - \omega_p)^2 + \Gamma^2},$$

where s , t are offset and scaling factors, ω_p is the bare phonon frequency, q is a dimensionless asymmetry parameter governing the line shape, and Γ is the half width at half maximum (HWHM) of the bare phonon that is the imaginary part of its self-energy.

The Fano parameters are found to be $\omega_p = 613.8 \text{ cm}^{-1}$, $q = -1.90$, and $\Gamma = 79.7 \text{ cm}^{-1}$ for F 3 (Y42); and $\omega_p = 609.8 \text{ cm}^{-1}$, $q = -2.68$, and $\Gamma = 60.8 \text{ cm}^{-1}$ for the chlorinated sample (CR-200). The Fano resonance $\omega_{\max} = \omega_p + \Gamma/q$ and antiresonance $\omega_{\min} = \omega_p - \Gamma q$ (curve extrema) are found, respectively, at 572 and 765 cm^{-1} for the pristine film F 3 and at 587 and 772 cm^{-1} for the chlorinated compound. There is a slight bare phonon frequency downshift and a relevant resonance frequency upshift ($\Delta\omega_p = -4 \text{ cm}^{-1}$ and $\Delta\omega_{\max} = +15 \text{ cm}^{-1}$) on going from pristine to chlorinated superconducting samples at 10 K . In the case of the chlorinated compound the electron-phonon coupling at 10 K is, in fact, stronger than in the pristine sample since the interaction potential $V = q\Gamma$ is higher and amounts -163 cm^{-1} whereas it is -151 cm^{-1} in the pristine material. We must also notice that we recorded at 676.4 nm a parallel-parallel polarized spectrum of film F 3 at room temperature which also exhibits a Fano shape since we were not able to fit it with one or several Lorentzians [Fig. 7(a)]. Fitting parameters were $\omega_p = 611.2 \text{ cm}^{-1}$, $q = -1.50$, and $\Gamma = 59 \text{ cm}^{-1}$, which give an ω_{\max} of 572 cm^{-1} . This yields a smaller interaction potential ($V = -88 \text{ cm}^{-1}$) than in the SC state and is consistent with a stronger electron-phonon coupling at low temperature. The corresponding room-temperature spectrum of CR-200 taken at 676.4 nm does not show any Fano shape and was fitted using a Lorentzian peaked at 582 cm^{-1} with a HWHM of 32.5 cm^{-1} [Fig. 7(b)].

The Fano fitting of the 580-cm^{-1} feature using very reasonable coupling parameters q confirms that it stems from the superconductor and not from some type of secondary phase. Consequently, this puts another evidence that the chlorinated crystallites optically investigated along this study were superconducting as also indicated by the extreme weakness of the Raman signal. In the frame of the phononic picture and from these calculations there seems to be no hardening or softening of the defect-induced mode of the pristine sample upon cooling, however, this mode broadens drastically ($+20 \text{ cm}^{-1}$) at 10 K whereas its intensity diminishes. There is a slight hardening ($+5 \text{ cm}^{-1}$) and strong broadening ($+28 \text{ cm}^{-1}$) of this mode for the chlorinated sample in the SC state with respect to the normal state. Absence of softening may indicate that there is no strong intermixing with the B_{1g} mode stemming from CuO_2 planes (337 cm^{-1}) which, in contrast, is known to soften below T_c .³⁷ The broadening of the defect-induced feature at 10 K is an anomalous behavior since the phonon linewidths usually decrease as an inverse exponential law with T that is the dependence is almost linear down to $50\text{--}100 \text{ K}$ with a plateau at low temperature. In addition this feature broadens much more below T_c ($20\text{--}30 \text{ cm}^{-1}$) than does

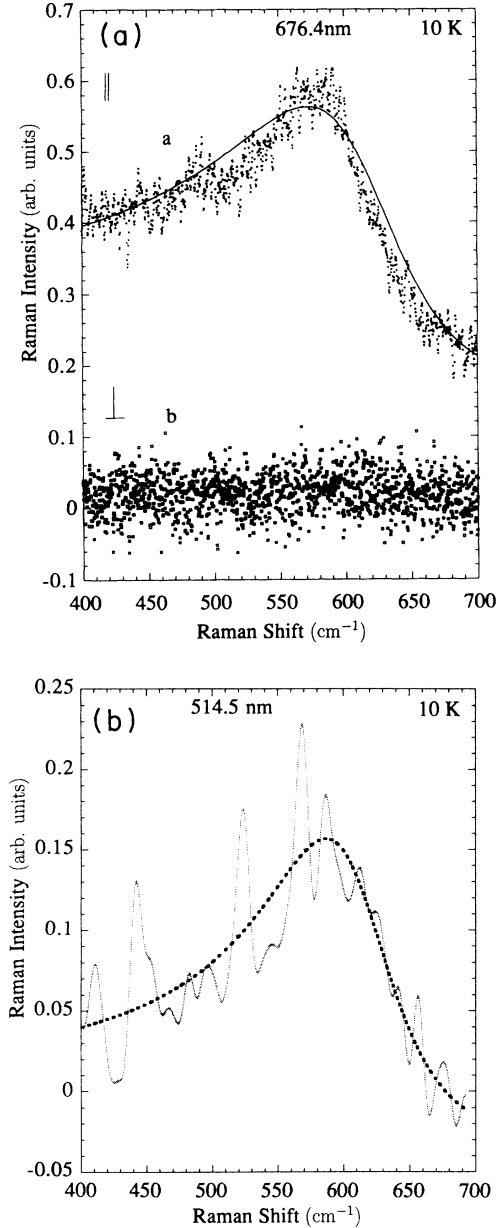


FIG. 6. (a) Low-temperature (10 K) Raman spectra of the pristine superconducting YBCO film F 3 (Y42) with strong oxygen disorder, polarization \parallel (a), and polarization \perp (b). Recorded with the 676.4-nm laser light, slightly smoothed with fast Fourier transform algorithm. (b) Low-temperature (10 K) Raman spectrum of the reduced chlorinated superconducting sample (CR-200) taken with the 514.5-nm laser line for unpolarized scattered light. Smoothed with the Savitsky-Golay algorithm. The lines at 521 and 588 cm^{-1} are laser plasma lines. The plain and dashed lines are the Fano line-shape fits of the experimental data. Fano parameters are discussed in the text.

the 337-cm^{-1} soft phonon (about 6 cm^{-1} between T_c and 10 K) and thus this broadening could be a sharp signature of a superconducting gap in both pristine and doped materials.³⁷ The broadening at low temperature of this defect-induced feature could also be related to a dynamic interaction with charge-transfer excitons recently evidenced in similar systems by Liu *et al.*³⁸ We note, however, that Γ is quite large and that the Fano fit is performed for a single phonon. Thus, we are cautious with its true nature. As we mentioned we may have observed multiple phonon scattering with several individual superimposed bands looking rather like a PDOS. The physical changes of line shape at low temperature are, however, unambiguous since the imaginary part of the self-energy of one or several phonons of this density obviously increases.

Finally, note that appearance of a relative strong band at 502 cm^{-1} for CR-150 and strong diminution of this

band for higher annealing temperatures T_a (Fig. 4, spectra *b*, *c*, and *d*) may show that chlorine doping promotes formation of $\text{YBa}_2\text{Cu}_3\text{O}_7$ cluster structures and domains at low temperature and that the oxygen disorder increases at higher T_a since the intensity and the HWHM of the 580-cm^{-1} band increases with T_a .

V. SUMMARY

In this paper we have investigated the modification of the oxygen sublattice and the phonon spectrum in pristine YBCO films and in modified YBCO ceramics annealed in chlorine atmosphere. The chlorine treatment was done for two series of compounds starting from the reduced form and the oxygenated form. The reduced chlorinated CR samples did not exhibit superconductivity, except for samples annealed at 200°C whereas the same annealing without chlorine in an inert atmosphere would not render a reduced sample superconducting at this temperature. Moreover, the superconductivity induced by chlorine treatment seems to appear only in a small temperature range, since CR samples annealed at 150°C and 250°C did not exhibit it. The situation is different in oxidized chlorinated CO compounds since superconductivity is only destroyed at 300°C . In these samples a reduction of the superconducting fraction f_S is observed, nevertheless f_S remains higher in the CO series than in the CR series for the same temperatures. This indicates that the intercalation process depends on the initial oxygen content. The systematic magnetization experiments reported here give some insights about the structure of these materials and the mechanism of superconductivity which is not solely driven by the charge transfer towards CuO chains but also likely by internal diffusion of oxygen from BaO planes towards partially filled CuO chains. In the CR series, we believe that chlorine intercalates in the barium layers vacancies rather than in the O(1) sites and promotes oxygen diffusion from O(4) sites towards adjacent copper layers in order to refill the CuO chains which trigger superconductivity at the critical chlorine substitution. In the CO series, most of the O(1) vacancies are already occupied by oxygen atoms before chlorine annealing, therefore chlorine should intercalate elsewhere in the lattice, likely in barium layers, but can induce also degradation of the superconductivity by taking the oxygen atoms out of CuO chains. Such a mechanism would be possible in the reduced chlorinated samples only when the CuO chains are refilled by internal diffusion, i.e., above the critical annealing temperature which triggers superconductivity. X-ray diffraction (XRD) patterns show that the chlorinated reduced series undergoes a tetragonal-orthorhombic transition for annealing temperatures above 200°C . Chlorine does not intercalate between YBCO layers since the *c*-cell parameter change is not sufficient to account for. Moreover, it is very likely from XRD and XPS results that the oxidation state of chlorine is between 0 and -1 . The Raman technique was used at our knowledge for the first time in the case of these chlorinated superconductors and a resonant feature was found near 580 cm^{-1} using three laser lines at 2.708, 2.410, and 1.834 eV. This band corresponds

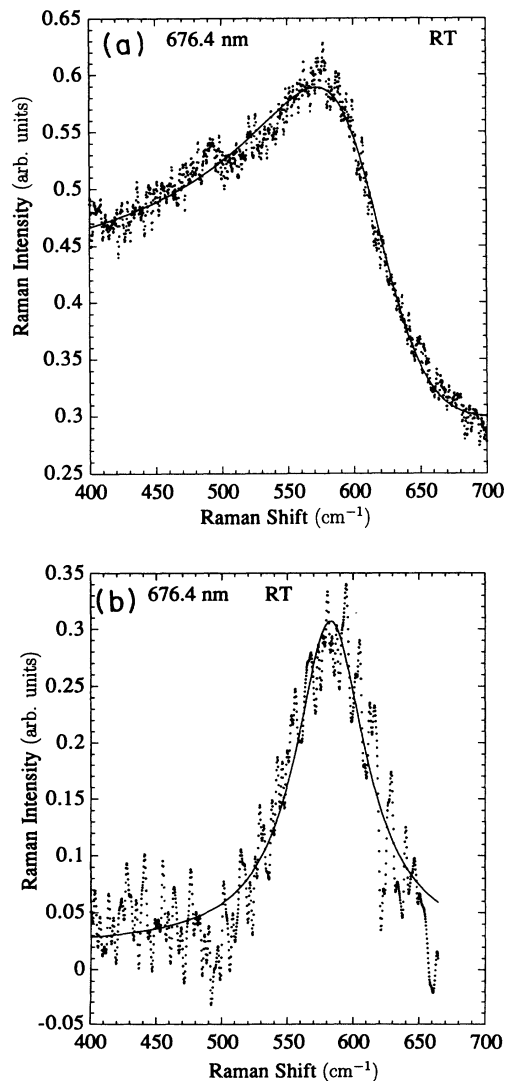


FIG. 7. Room-temperature Raman spectra (676.4 nm) of film F 3 (a) and CR-200 sample (b). The plain lines are fits of the spectra.

well to a density of phonon states centered at the position where vibrations of oxygen vacancy defects of CuO chains and BaO planes are expected. It is therefore possible that apex oxygen O(4) atoms would be substituted for chlorine atoms for all chlorinated samples. The experiments carried out at low temperature have shown characteristic Fano line shapes for the 580-cm^{-1} feature and unusual strong broadening in the SC state suggesting in-

teraction with electronic excitations traveling from CuO_2 planes to CuO chains.

ACKNOWLEDGMENTS

Laboratoire de Physique Cristalline is Unité Mixte de Recherche au CNRS No. 110. Laboratoire de Chimie des Solides is Unité Mixte de Recherche au CNRS No. 110.

- ¹Yu. A. Osipyan, O. V. Zharikov, N. S. Sidorov, V. I. Kulakov, D. N. Mogilyanskii, R. K. Nikolaev, S. Sh. Shekhtman, O. A. Volegova, and I. M. Romanenko, *Pis'ma Zh. Eksp. Teor. Fiz.* **458**, 225 (1988) [*JETP Lett.* **48**, 246 (1988)].
- ²Yu. T. Pavlyukhin, A. P. Nemudry, N. G. Khainovsky, and V. V. Boldyrev, *Solid State Commun.* **72**, 107 (1989).
- ³H. B. Radousky, R. S. Glass, D. Back, A. H. Chin, M. J. Fluss, J. Z. Liu, W. D. Mosly, P. Klavins, and R. N. Shelton, *IEEE Trans. Magn.* **27**, 2512 (1991).
- ⁴A. M. Stewart, J. S. Anderson, J. G. Thompson, B. G. Hyde, R. L. Withers, J. D. Fitzgerald, M. S. Paterson, and J. Bitmead, *Mater. Chem. Phys.* **20**, 397 (1988).
- ⁵S. Myhra, P. C. Healy, C. F. Jones, H. E. Bishop, P. Marriott, J. C. Riviere, and A. M. Stewart, *Mater. Chem. Phys.* **25**, 135 (1990).
- ⁶M. Evain (unpublished).
- ⁷M. Ezrahi, L. Brohan, and M. Ganne, *Eur. J. Solid State Inorg. Chem.* **30**, 35 (1993); M. Ezrahi, Thèse de Doctorat, Nantes, 1993.
- ⁸G. Garz, E. Faulques, G. Le Roux, J. Schneck, and C. Gonzalez, *Proceedings of the European Conference on Applied Superconductivity*, Göttingen, 1993 (Springer-Verlag, Berlin, 1993).
- ⁹G. Burns, F. H. Dacol, C. Feild, and F. Holtzberg, *Solid State Commun.* **77**, 367 (1991).
- ¹⁰H. Kuzmany, E. Faulques, M. Matus, and S. Pekker, in *Studies of High T_c Superconductors*, edited by A. V. Narlikar (Nova Science, New York, 1989).
- ¹¹J. Rimmel, O. Meyer, J. Geek, J. Reiner, G. Linker, A. Erb, and G. Müller-Vogt, *Phys. Rev. B* **48**, 16 168 (1993).
- ¹²T. P. Nguyen, E. Faulques, and P. Molinié, *Phys. Rev. B* **48**, 12 989 (1993).
- ¹³E. Faulques, P. Molinié, P. Berdahl, T. P. Nguyen, and J. L. Mansot, *Physica C* **219**, 297 (1994).
- ¹⁴P. Steiner, V. Kisinger, I. Sander, S. Siegwart, C. Huebner, and C. Politis, *Z. Phys. B* **67**, 19 (1987).
- ¹⁵T. P. Nguyen, P. Dupouy, and E. Faulques, *Eur. J. Solid State Inorg. Chem.* **27**, 689 (1990).
- ¹⁶See for example, H. Fjellwag, P. Karen, A. Kjekshus, and J. K. Grepstad, *Solid State Commun.* **64**, 917 (1987).
- ¹⁷D. E. Fowler, C. R. Brundle, J. Lercjak, and F. Holtzberg, *J. Electron. Spectrosc. Relat. Phenom.* **52**, 323 (1990).
- ¹⁸R. P. Vasquez, in *Materials Science Series*, edited by J. J. Pouch, S. A. Alterovitz, and R. Romanovsky (Trans Tech, Aedermannsdorf, Switzerland, 1992).
- ¹⁹J. H. Weaver, H. M. Meyer, J. T. Wagener, D. M. Hill, Y. Gao, D. Peterson, Z. Fisk, and A. J. Arko, *Phys. Rev. B* **38**, 4668 (1988).
- ²⁰D. T. Clark and H. T. Thomas, *J. Polym. Sci.: Polym. Chem. Ed.* **16**, 791 (1978).
- ²¹*Handbook of X-ray Photoelectron Spectroscopy*, edited by C. D. W. M. Wagner, W. M. Riggs, L. E. Davis, J. F. Moulderand, G. E. Muellenberg (Perkin Elmer, Eden Prairie, 1978).
- ²²H. Jaeger, S. Hofman, G. Kaiser, K. Schulze, and G. Petsow, *Physica* **155**, 133 (1988).
- ²³R. P. Vasquez, *J. Electron. Spectrosc. Relat. Phenom.* **56**, 217 (1991).
- ²⁴E. Faulques, P. Dupouy, and S. Lefrant, *J. Phys. I (France)* **1**, 901 (1991).
- ²⁵M. Iliev, C. Thomsen, V. Hadjiev, and M. Cardona, *Phys. Rev. B* **47**, 12 341 (1993).
- ²⁶R. Feile, *Physica C* **159**, 1 (1989).
- ²⁷X. K. Chen, E. Altendorf, J. C. Irwin, R. Liang, and W. N. Hardy, *Phys. Rev. B* **48**, 10 530 (1993).
- ²⁸V. G. Hadjiev, C. Thomsen, A. Erb, G. Mueller-Vogt, M. R. Koblischka, and M. Cardona, *Solid State Commun.* **80**, 643 (1991).
- ²⁹A. Erle, S. Blumenroeder, E. Zirngiebl, and G. Guentherodt, *Solid State Commun.* **73**, 753 (1990).
- ³⁰G. Burns, F. H. Dacol, C. Feild, and F. Holtzberg, *Solid State Commun.* **75**, 893 (1990).
- ³¹M. V. Belousov, I. V. Ignat'ev, N. V. Orekhova, and V. Yu Davydov, *Fiz. Tverd. Tela (Leningrad)* **34**, 2804 (1992) [*Sov. Phys. Solid State* **34**, 1500 (1992)].
- ³²I. V. Gasparov, V. D. Kulakovskii, V. B. Timofeev, and V. Ya Sherman, *Zh. Eksp. Teor. Fiz.* **100**, 1681 (1991) [*Sov. Phys. JETP* **73**, 929 (1991)].
- ³³H. Kuzmany, M. Matus, E. Faulques, S. Pekker, G. Hutiray, E. Zsoldos, and L. Mihaly, *Solid State Commun.* **65**, 1343 (1988).
- ³⁴B. Guettler, E. Salje, P. Freeman, J. Blunt, M. Harris, T. Duffield, C. D. Ager, and H. P. Hughes, *J. Phys. C* **2**, 8977 (1990).
- ³⁵B. Renker, F. Gompf, E. Gering, D. Ewert, H. Rietschel, and A. Dianoux, *Z. Phys. B* **73**, 309 (1988).
- ³⁶U. Fano, *Phys. Rev.* **124**, 1866 (1961).
- ³⁷C. Thomsen, in *Light Scattering in High T_c Superconductors*, edited by M. Cardona and G. Guentherodt, *Topics in Applied Physics Vol. 68* (Springer-Verlag, Berlin, 1991), pp. 285–359, and references therein.
- ³⁸R. Liu, D. Salamon, M. V. Klein, S. L. Cooper, W. C. Lee, S. W. Cheong, and D. M. Ginsberg, *Phys. Rev. Lett.* **71**, 3709 (1993).